Science Translational Medicine
AAAS

Supplementary Materials for

T cell responses to SARS-CoV-2 infection and vaccination are elevated in B cell deficiency and reduce risk of severe COVID-19

Reza Zonozi *et al.*

Corresponding author: John L. Niles, jlniles@mgh.harvard.edu; Gaurav D. Gaiha, ggaiha@mgh.harvard.edu

Sci. Transl. Med. **15**, eadh4529 (2023)
DOI: 10.1126/scitranslmed.adh4529

The PDF file includes:

Other Supplementary Material for this manuscript includes the following:

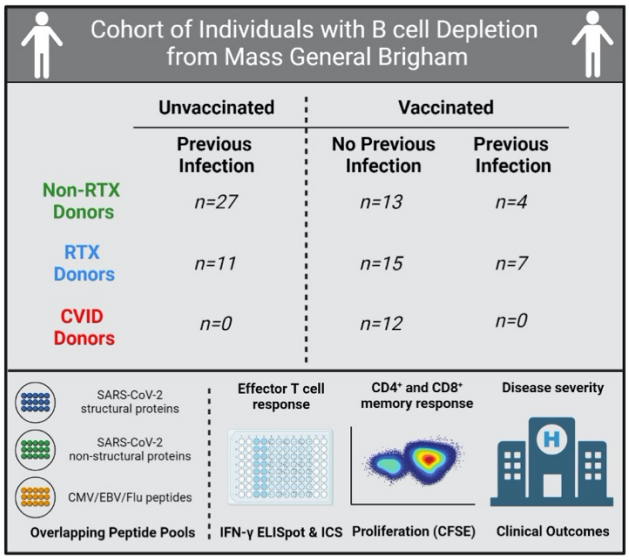

Figure S1. Study design and characteristics of cohort evaluated for immunologic assessments. Enrolled participants (n=89) were stratified according to whether they had documented SARS-CoV-2 infection and vaccination status and whether they had received RTX treatment or had underlying CVID. Total ($CD4^+$ and $CD8^+$) effector T cell reactivity to overlapping peptide pools from wildtype SARS-CoV-2 structural, accessory and non-structural proteins was assessed by IFN-γ ELISpot. $CD4^+$ and $CD8^+$ memory T cell responses to spike protein and non-spike protein peptide pools was assessed by CFSE-based proliferation assay. Numbers for each group are shown. Schematic of the study created with Biorender.com.

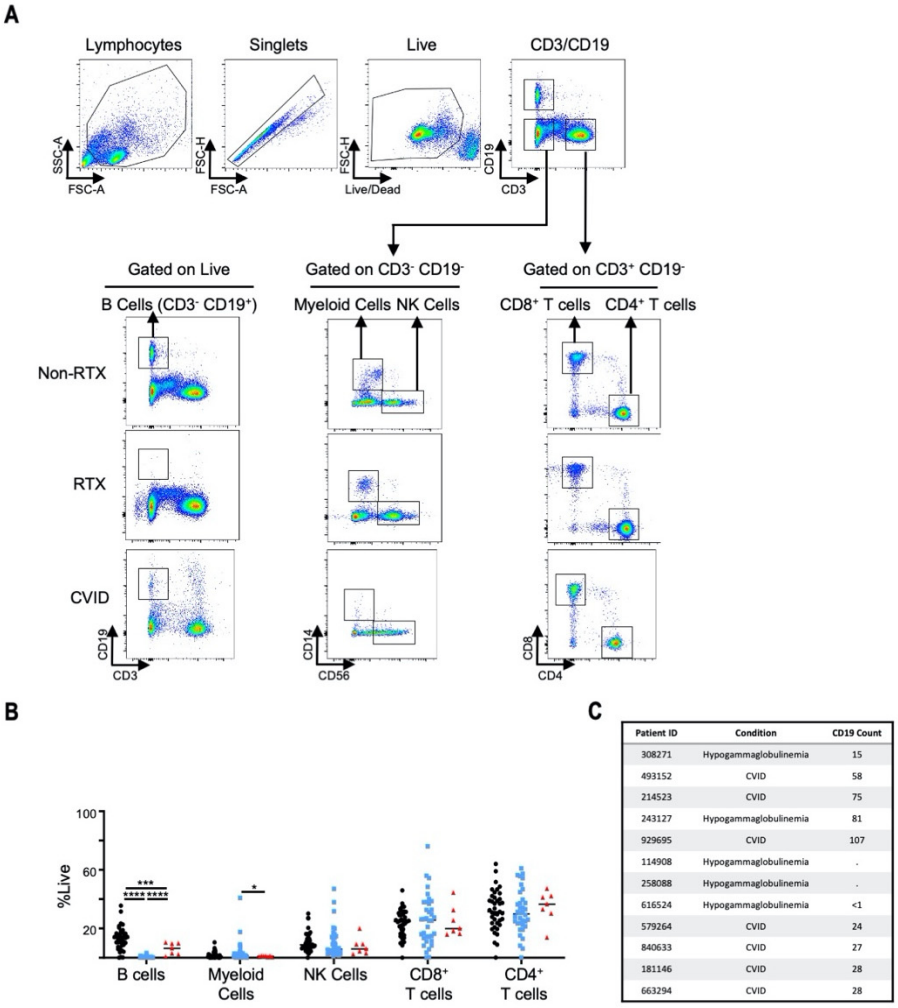

Patient ID	Condition	CD19 Count
308271	Hypogammaglobulinemia	15
493152	CVID	58
214523	CVID	75
243127	Hypogammaglobulinemia	81
929695	CVID	107
114908	Hypogammaglobulinemia	.
258088	Hypogammaglobulinemia	.
616524	Hypogammaglobulinemia	<1
579264	CVID	24
840633	CVID	27
181146	CVID	28
663294	CVID	28

Fig S2. Immune phenotyping of peripheral blood mononuclear cell (PBMC) specimens from Non-rituximab (RTX)-treated individuals, RTX-treated individuals, and individuals with common variable immune deficiency disease (CVID). (**A**) Gating strategy for immune phenotyping and quantification of immune cell subsets in PBMC specimens. FSC, forward scatter; SSC, side scatter; A, area; H, height; NK cells, natural killer cells. (**B**) Comparative frequencies of indicated immune cell subtypes in non-RTX-treated healthy controls (black, n=39), RTX-treated individuals (blue, n=36) and individuals with CVID (red, n=7). (**C**) Underlying medical condition and CD19 count of individuals with CVID evaluated in this study. Differences between groups were evaluated using the Kruskal-Wallis test with Dunn's post hoc analyses for correction of multiple comparisons. Bars represent median values. Data are biological replicates. Calculated p values are presented as follows: *$p < 0.05$; ***$p < 0.001$; ****$p < 0.0001$.

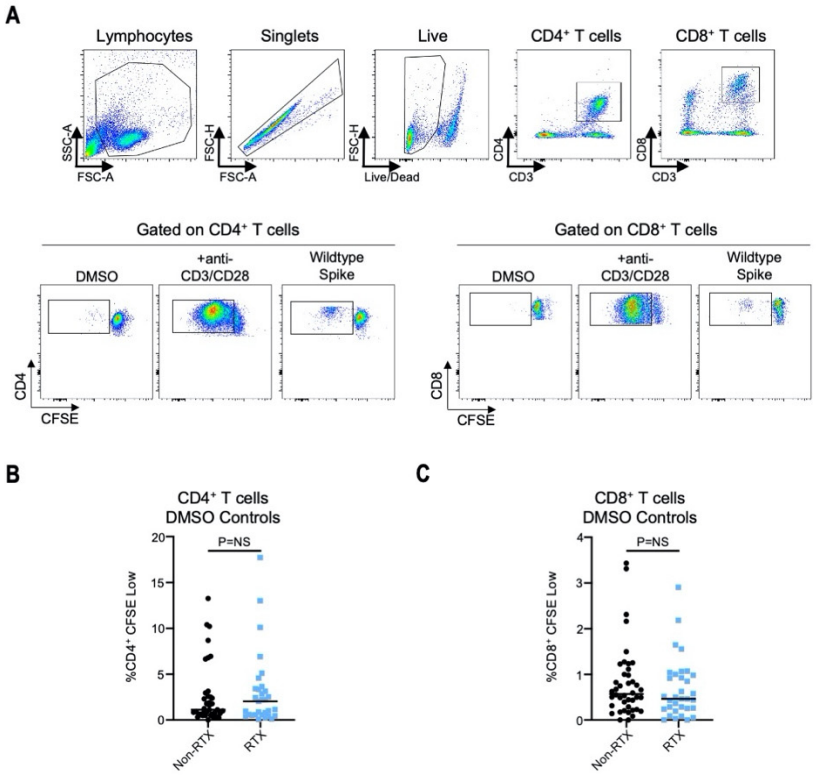

Fig. S3. Gating strategy for carboxyfluorescein succinimidyl ester (CFSE) proliferation assay. (**A**) Representative gating strategy for identification of proliferating $CD3^+$ $CD4^+$ and $CD3^+$ $CD8^+$ CFSE low T cells in response to peptide pools of interest. The gate establishing the frequency of CFSE low $CD4^+$ or $CD8^+$ cells was chosen based on minimizing responses in two negative-control (DMSO) wells and verified using positive control (CD3/CD28) wells. (**B and C**) Negative control (DMSO) CFSE low $CD4^+$ (**B**) or CFSE low $CD8^+$ (**C**) T cells are shown for all Non-RTX (n=42) and RTX-treated (n=33) individuals evaluated in the study. Statistical comparisons were made by non-parametric Mann-Whitney U test. Bars represent median values. Data are biological replicates. NS, not significant.

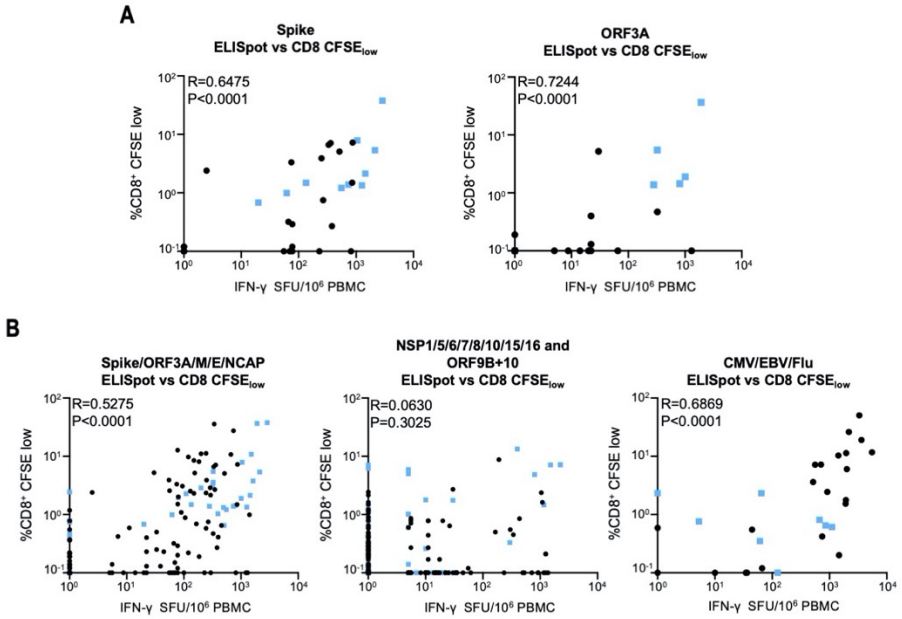

Fig. S4. Correlation of ELISpot and CD8$^+$ CFSE-based proliferation data for prior infected individuals. (**A**) Scatter plots of the magnitude of ELISpot and CD8$^+$CFSE$_{low}$ responses in Non-RTX (black, n=24) and RTX-treated (blue, n=10 for spike protein, n=6 for open reading frame (ORF) 3A) individuals following spike protein or ORF3A peptide pool stimulation. IFN-γ, interferon-γ; SFU, spot-forming unit. (**B**) Scatter plots of the magnitude of ELISpot and CD8$^+$CFSE$_{low}$ responses in Non-RTX (black, n=24) and RTX-treated (blue, n=10 for spike, n=8 for CEF, n=6 for remaining conditions) individuals following Spike/ORF3A/membrane (M)/envelope (E)/nucleocapsid (NCAP), non-structural protein (NSP)1/5/6/7/8/10/15/16 and ORF9B+10, or cytomegalovirus (CMV)/Epstein-Barr virus (EBV)/Influenza (Flu) (CEF) peptide pool stimulation. Correlations were calculated by Spearman's rank correlation coefficient.

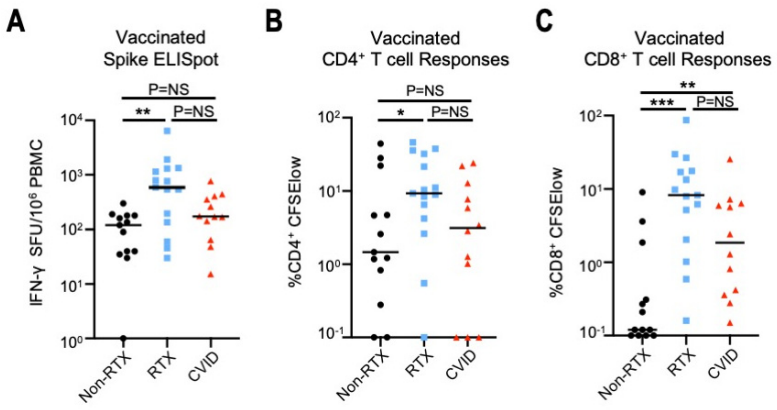

Fig. S5. Comparison of spike protein-specific T cell responses in vaccinated Non-RTX, RTX-treated and CVID individuals. (A to C) Comparison of spike protein-specific IFN-γ ELISpot T cell responses **(A)**, spike protein-specific proliferative $CD4^+$ T cell responses **(B)**, and spike protein-specific proliferative $CD8^+$ T cell responses **(C),** non-RTX-treated individuals (black, n=13), RTX-treated individuals (blue, n=15) and individuals with CVID (red, n=12) following severe acute respiratory syndrome coronavirus 2 (SARS-CoV-2) vaccination. Differences between groups were evaluated using the Kruskal-Wallis test with Dunn's post hoc analyses for correction of multiple comparisons. Bars represent median values. Data are biological replicates. Calculated p values are presented as follows: *$p < 0.05$; **$p < 0.01$; ***$p < 0.001$; NS, not significant.

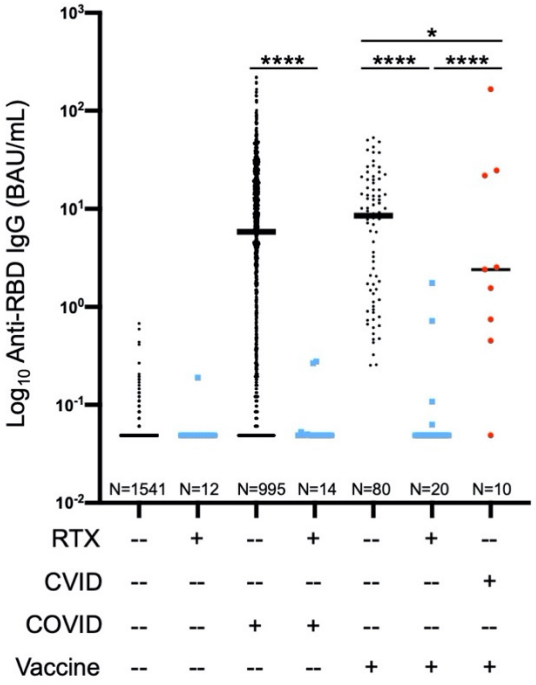

Fig. S6. Anti-receptor binding domain (RBD) antibody concentrations in non-RTX-treated individuals, RTX-treated individuals and individuals with CVID. Comparison of anti-RBD IgG concentrations (log_{10} BAU/mL) in non-RTX-treated individuals (black), RTX-treated individuals (blue), and individuals with CVID (red) following SARS-CoV-2 infection or vaccination. Differences between groups were evaluated using Kruskal-Wallis test with Dunn's post hoc analyses for correction of multiple comparisons. Bars represent median values. Data are biological replicates. Calculated p values are presented as follows: *$p < 0.05$; ****$p < 0.0001$.

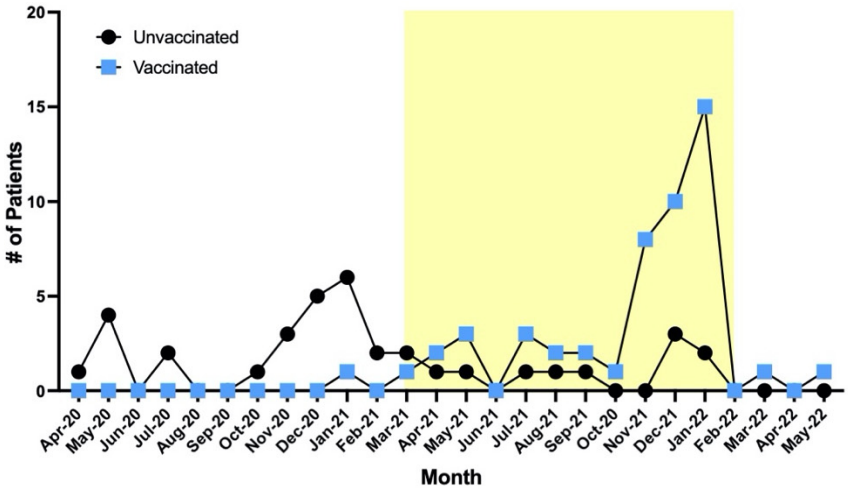

Fig. S7. Timing of SARS-CoV-2 infections for RTX-treated unvaccinated and vaccinated individuals evaluated in the clinical outcomes analysis. The number of RTX-treated unvaccinated (n=36, black) and vaccinated (n=50, blue) individuals, which lacked detectable spike protein-specific antibodies and were evaluated in the clinical outcomes analysis, that were infected each month between April 2020 and May 2022. The region in yellow represents the period of overlap where both unvaccinated and vaccinated participants had new infections (March 2021 to February 2022).

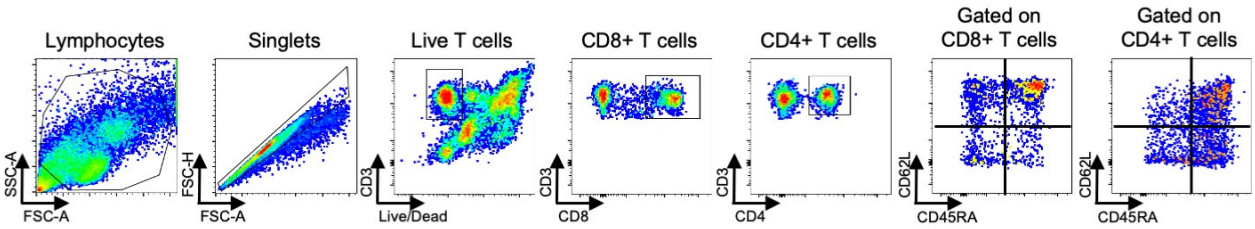

Fig. S8. Gating strategy for T cell memory markers. Representative gating strategy for identification of different memory subsets of $CD3^{+}CD4^{+}$ and $CD3^{+}CD8^{+}$ T cells. Gating established the frequency of naïve ($CD45RA^{+}$ $CD62L^{+}$), central memory ($CD45RA^{-}$ $CD62L^{+}$), effector memory ($CD45RA^{-}$ $CD62L^{-}$), and terminally differentiated ($CD45RA^{+}$ $CD62L^{-}$) T cells.

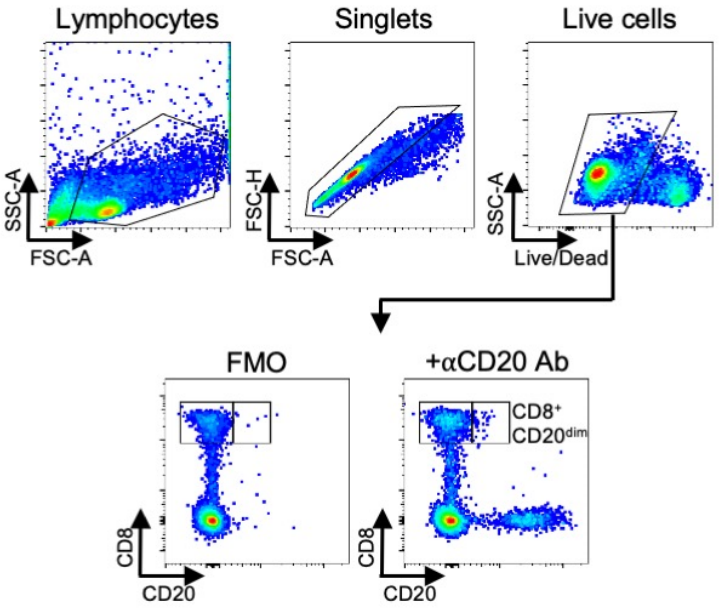

Fig. S9. Gating strategy for $CD8^{+}CD20^{dim}$ T cells. Representative gating strategy for identification of $CD8^{+}CD20^{dim}$ T cells. Data from fluorescence minus one (FMO) and αCD20 antibody (Ab) surface staining are displayed for a non-RTX-treated individual.

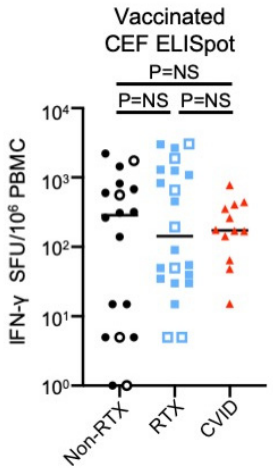

Fig. S10. Comparison of CEF-specific T cell responses in vaccinated Non-RTX, RTX-treated and CVID individuals. Comparison of CEF-specific IFN-γ ELISpot T cell responses in non-RTX-treated individuals (black, n=18), RTX-treated individuals (blue, n=22) and individuals with CVID (red, n=12) following severe acute respiratory syndrome coronavirus 2 (SARS-CoV-2) vaccination. Open symbols represent individuals with hybrid immunity. Differences between groups were evaluated using the Kruskal-Wallis test with Dunn's post hoc analyses for correction of multiple comparisons. Bars represent median values. Data are biological replicates. Calculated p values are presented as follows: NS, not significant.

Table S1. Baseline characteristics of non-RTX-treated individuals, RTX-treated individuals, and individuals with CVID evaluated for immune assessments.

Characteristic	Non-RTX, (N=44)	RTX, (N=33)	CVID, (N=12)
Age	48 (40,56)	56 (43,65)	55 (41,68)
Sex			
Female	21 (47%)	17 (52%)	9 (75%)
Male	23 (53%)	16 (48%)	3 (25%)
Prior Severe Acute Respiratory Syndrome Coronavirus 2 (SARS-CoV-2) Infection			
Polymerase Chain Reaction/Antibody confirmed prior infection	31 (70%)	22 (67%)	0 (0%)
No prior infection	13 (30%)	11 (33%)	12 (100%)
Time to sample acquisition following SARS-CoV-2 infection	196 (74,315)	146 (80,283)	0 (0,0)
Vaccine Type			
BNT162b2	10 (22%)	10 (24%)	7 (58%)
mRNA1273	7 (15%)	12 (29%)	5 (42%)
Time to sample acquisition following vaccination	24 (18,40)	47 (28,136)	90 (43,188)
Reason for Rituximab Treatment			
Anti-neutrophilic cytoplasmic antibody vasculitis	N/A	12 (43%)	N/A
Nephrotic Syndrome	N/A	1 (4%)	N/A
Membranous nephropathy	N/A	2 (7%)	N/A
Fibrillary glomerulonephritis	N/A	1 (4%)	N/A
Lupus nephritis	N/A	6 (21%)	N/A
Idiopathic Membranoproliferative Glomerulonephritis	N/A	2 (7%)	N/A
Focal segmental glomerulosclerosis	N/A	2 (7%)	N/A
Interstitial Lung Disease	N/A	3 (11%)	N/A
Rheumatoid Arthritis	N/A	4 (14%)	N/A
Time to sample acquisition following Rituximab administration	N/A	203 (127,288)	N/A
B cell count at time of sampling	---	0 (0,40)	28 (25,71)
T cell count			
CD3 count	---	1124 (886,1964)	---
CD4 count	---	768 (606,961)	---
CD8 count	---	489 (250,783)	---
Individuals with Pre- and Post-Vaccine Specimens	3	5	---

Data shown as Median (Interquartile Range); n (%); Range

Table S2. Baseline characteristics of individuals evaluated for clinical outcomes analysis.

Characteristic	Unvaccinated, N=36	Vaccinated, N=74
Age	55 (36, 63)	58 (46, 67)
Female Sex	19 (53%)	45 (61%)
Body Mass Index (BMI)	28 (24, 34)	28 (26, 34)
Anti-spike protein antibody level		
Undetecable	36 (100%)	50 (67%)
Minimal (< 20 units)	0 (0%)	9 (12%)
Moderate (> 20 units)	0 (0%)	15 (21%)
Autoimmune.disease		
Anti-neutrophilic cytoplasmic antibody vasculitis	25 (69%)	47 (65%)
Focal segmental glomerulosclerosis	3 (8.3%)	0 (0%)
Immune complex glomerulonephritis not otherwise specified	1 (2.8%)	1 (1.4%)
Interstitial lung disease	0 (0%)	2 (2.8%)
Membranous nephropathy	3 (8.3%)	4 (4.2%)
Minimal change disease	1 (2.8%)	5 (6.9%)
Mixed connective tissue disease	0 (0%)	1 (1.4%)
Monoclonal gammopathy of renal significance	0 (0%)	1 (1.4%)
Retinal vasculitis	0 (0%)	1 (1.4%)
Rheumatoid arthritis	0 (0%)	3 (4.2%)
Systemic lupus erythematosus	2 (5.6%)	7 (8.3%)
Urticarial vasculitis	1 (2.8%)	0 (0%)
Positive Test Date	2020-04-15 to 2022-01-09	2021-03-29 to 2022-05-27
Coronavirus Disease 2019 Symptom Severity		
Mild - home	12 (33%)	52 (70%)
Moderate, Extended Emergency Department or Hospitalized	4 (11%)	7 (9.5%)
Severe hospitalized	13 (36%)	4 (5.4%)
Critical - Intensive Care Unit with intubated, or Extracorporeal Membrane		
Oxygenation, or proning with high flow O2	2 (5.5%)	3 (4.1%)
Death	5 (14%)	8 (11%)
Evusheld	0 (0%)	0 (0%)
Sotrovimab	0 (0%)	0 (0%)
Remdesivir	0 (0%)	0 (0%)
Paxlovid	0 (0%)	0 (0%)
Dexamethasone	0 (0%)	0 (0%)
Other Monoclonal Antibody Treatment	0 (0%)	0 (0%)
Obesity (BMI > 30)	13 (36%)	28 (38%)

Data shown as Median (Interquartile Range); n (%); Range

Table S3. Correlates of moderate/severe/critical/fatal coronavirus disease 2019 (COVID-19) in unvaccinated and vaccinated RTX-treated individuals with no detectable anti-spike protein antibody response between March 2021 and February 2022 during an overlapping period of new infections. Results of multivariable regression are shown for unvaccinated (n=12) and vaccinated RTX-treated individuals (n=46) with infections from March 2021 to February 2022 (**table S1**). CI, confidence interval.

Characteristic	Adjusted Odds of Moderate/Severe/Critical/Fatal COVID-19	95% Confidence Interval	Adjusted P-value
Age (per 10-year increase)	2.22	1.32-4.27	0.007
Sex (Male vs. Female)	2.96	0.75-13.9	0.14
Obesity (BMI > 30)	8.15	1.89-45.3	0.009
Completed Vaccination	0.07	0.01-0.46	0.013

Data file S1. Raw, individual-level data for experiments where n<20.